East European Journal of Physics. 3. 293-297 (2024)
DOI:10.26565/2312-4334-2024-3-30 ISSN 2312-4334

AN OPTIMIZED ULTRASONIC SPRAY PYROLYSIS DEVICE FOR THE PRODUCTION OF METAL OXIDE FILMS AND THEIR MORFOLOGY

Sirajidin S. Zainabidinov[a], Akramjon Y. Boboev[a,b], Nuritdin Y. Yunusaliyev[a], Jakhongir N. Usmonov[a]
[a]*Andijan State University named after Z.M. Babur, Andijan, Uzbekistan*
[b]*Institute of Semiconductor Physics and Microelectronics, National University of Uzbekistan, Tashkent, Uzbekistan*
**Corresponding Author e-mail: aboboevscp@gmail.com*
Received June 30, 2024; revised July 27, 2024; accepted August 1, 2024

In this work, we developed an optimized ultrasonic spray pyrolysis device for obtaining metal oxide films. The key benefit of this facility lies in its cost-effectiveness and its ability to consistently coat extensive surfaces without sacrificing the integrity of the semiconductive films, thus streamlining the manufacturing process of semiconductor films. The resulting films exhibit the following attributes: the thickness of the deposited layer is approximately 400 nm, while the diameters of $ZnO_{1-x}S_x$ nanocrystals range from 50 to 200 nm, oriented perpendicular to the crystallographic orientation (111). In the production of nanorods, the average height is estimated to be approximately 30-50 nm, with a density of 2.9×10^{11} cm^{-2} being indicated.
Keywords: *Film; Space group; Subcrystal; Nanocrystal; Quantum size effect; Lattice parameter; Transparent electronics; Band gap*
PACS: 78.30.Am

1. INTRODUCTION

Currently, wide-bandgap semiconductors such as zinc oxide (ZnO) and gallium nitride (GaN) are considered the most promising basic materials for the development of optoelectronic devices with predominant emission in the blue and ultraviolet spectral ranges. The bandgap energies (at 300 K) of Eg ~ 3.37 eV and 3.39 eV for ZnO and GaN, respectively, make them suitable for such applications [1,2]. GaN-based structures are already widely used for light sources (semiconductor light-emitting diodes and lasers) in the blue and ultraviolet regions of the optical spectrum. However, ZnO appears to be an equally promising semiconductor material for use in light-emitting devices as gallium nitride. It is known that ultraviolet emission in ZnO is due to excitonic recombination [3]. In the case of exciton photogeneration, ZnO allows for very low threshold power of optical pumping at 24 kW/cm^2. For comparison, excitons in gallium nitride are thermally unstable at room temperature (Eexc., GaN = 25 meV), and forced emission in the edge region is usually obtained through the recombination of electron-hole plasma, which results in significant threshold power values of optical pumping at 1.2 MW/cm^2 (almost 2 orders of magnitude higher than in ZnO), and as a result, the need to use micrometer-sized laser resonators. This is precisely why, in order to increase the exciton binding energy and reduce the generation threshold in the creation of semiconductor lasers and LEDs based on GaN (the main material for producing semiconductors in the short-wavelength range), more complex and expensive structures with quantum wells are used.

An important advantage of using ZnO structures is their low cost, as zinc makes up 0.1% of the Earth's crust, and the much lower toxicity of zinc compared to many other materials used in the semiconductor industry. The potential of using ZnO-based structures also lies in the possibility of expanding the optical emission range using solid solutions based on ZnO, such as ZnMgO and ZnCdO, etc. [4-5].

In this study, zinc oxide films were obtained using the ultrasonic spray pyrolysis method, and the optimal conditions of the technology were determined.

The conventional method of pulverization followed by pyrolysis has long been known and widely used. In this particular technique, the combination of pulverization with ultrasonic atomization, with the appropriate selection of synthesis conditions, substrate materials, and reagent concentrations, ensures the formation of ZnO films with acceptor-type doping [6-8]. Therefore, the most promising approaches currently considered are - the synthesis or doping of zinc oxide under significantly non-equilibrium conditions; annealing under a substance film with inadequate solubility of compound components; and annealing of crystals in an atmosphere of atomic halogen. In this case, to a certain extent, all three of these approaches are implemented. For example, during the pyrolysis of ultra-thin films of zinc nitrate and/or acetate solutions on the substrate surface, significantly non-equilibrium thermodynamic conditions arise, leading among other things to the formation of atomic oxygen and sulfur, as well as groups O-S, Zn-O-S, etc., aligning in the growing film. By using (selecting) substrates with different solubilities (or different diffusion coefficients) of ZnO and S atoms, it is possible, during post-annealing, to control the relative (and absolute) rates of "healing" of various defects. In this case, to a certain extent, all three of these approaches are implemented. For example, during the pyrolysis of ultra-thin films of zinc nitrate and/or acetate solutions on the substrate surface [9], significantly non-equilibrium thermodynamic conditions arise, leading among other things to the formation of atomic oxygen and sulfur, as well as O-S, Zn-O-S, and so on, groups that are arranged in the growing film. By using (selecting) substrates with different solubility (or different diffusion

Cite as: S.S. Zainabidinov, A.Y. Boboev, N.Y. Yunusaliyev, J.N. Usmonov, East Eur. J. Phys. 3, 293 (2024), https://doi.org/10.26565/2312-4334-2024-3-30

coefficients) of ZnO and S atoms, it is possible, during the post-annealing process, to control the relative (and absolute) rates of "healing" of different defects.

2. DESCRIPTION OF AN OPTIMIZED ULTRASONIC SPRAY PYROLYSIS DEVICE

To verify the production of p-type ZnO, an ultrasonic setup was created for the synthesis of ZnO, as schematically shown in (Figure. 1). The setup consisted of an ultrasonic generator (1), evaporator (2), cylindrical quartz glass (3), double-layer cooling flask (4), additional liquid inlet pipe (5), gas inlet pipe (6), pump (7), gas outlet pipe (8), substrate (9), valve (for pump control) (10), valve (for pyrolysis time control) (11), tube clamp (12), stand with scale (for adjusting the distance between the spray head and the substrate) (13), heating platform (14), ring tube with holes at equal distances (15), water-filled container for filtration (16), thermocouple (17), glass transparent cover (18), cylindrical hollow body (19). Additionally, Figure 2 shows the diagram of the cylindrical hollow body device, where the water storage volume (20), spray head (21), and liquid outlet tube (22) are located.

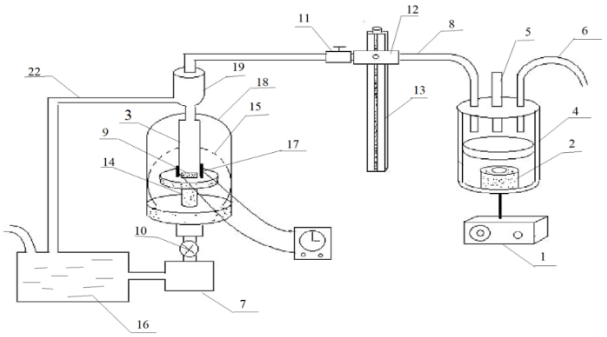

Figure 1. Optimized ultrasonic spray pyrolysis device for the production of metal oxide films

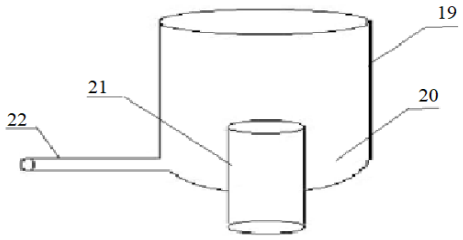

Figure 2 Diagram of the structure of a cylindrical hollow body

The ultrasonic generator emits a high-frequency pulse and sends it to the evaporator (ceramic or quartz piezoelectric material). As a result, the vibration is transmitted to the liquid (water) in the two-layer cooling flask. Upon the supply of the necessary chemical precursor through the additional outlet pipe (5) for the liquid into the two-layer cooling flask (4), the evaporation of the chemical precursor will begin. The pump (7) pulls the gas through the outlet pipe (8) to the substrate (9) from the vapor formed in the two-layer cooling flask (4) and the air passing through the gas inlet pipe (6) by means of a ring pipe with holes at equal distances (15). The captured air and chemical precursor vapors enter the cylindrical hollow housing (19) until they reach the substrate.

Through the use of a spray head (21), clean vapors are directed onto the substrate (9), while excess liquid, which negatively impacts the quality of the film, is collected in a water storage volume (20). The liquid collected in the water storage volume (20) is transferred through a liquid discharge pipe (22) into a container filled with water for filtration (16), where excess gases are also directed through a ring pipe with evenly spaced holes (15). Adjustments to the pump's (7) thrust force are made using a crane (10), while the dwell time and coating level are regulated with an additional valve (11). The distance between the substrate and the spray head is adjusted by vertically moving the gas exhaust pipe (8) on a stand with a scale (13), which is secured by a clamp (12). The substrate (9) and the vapors near it are heated by a heating platform (14). The necessary vapor is deposited as a layer on the substrate (9). Temperature is monitored and regulated by a thermocouple (17). The presence of a transparent glass cover (18) ensures that the process takes place in enclosed conditions.

Zinc acetate aqueous solutions were used as precursors for the deposition of ZnO films. To conduct doping, fatty elements were added to the zinc acetate aqueous solutions in the corresponding concentration, such as thiourea to obtain p-type conductivity ZnO or ammonium acetate to obtain n-type conductivity [10-12]. As a result of ultrasonic treatment of these solutions, the transition of the liquid to vapor occurred without significant heating of the liquid. The vapor formed as a result of ultrasonic treatment was deposited onto the substrate.

The substrate was heated to temperatures sufficient for the thermal decomposition of precursors, and on its surface, deposition occurred with the formation of ZnO film.

The formulas (1) represent the chemical reactions occurring during the synthesis of films:

$$4Zn(CH_3COO)_2+10H_2O+4CH_4N_2S \rightarrow 4ZnO(S)+8NH_3\uparrow+9CH_3COOH+2CO_2\uparrow. \quad (1)$$

3. MORPHOLOGY OF METAL OXIDE FILMS BY SPRAY PYROLYSIS DEVICE

To investigate the surface relief of ZnO1-xSx thin films, an atomic force microscope (AFM) "Solver-NEXT" SPM 9700HT (Shimadzu) was used. It is known that when calculating the profile obtained by the AFM method, the maximum depth of probe deviation is taken as zero. When studying a system with a low density of islands and a small filling coefficient of the heterostructure material, there is a high probability of the probe hitting the film surface and, therefore,

the correct choice of the zero level. The ratio of the average coating thickness calculated from the obtained AFM profile to the thickness measured in the experiment can be taken as a criterion for the correctness of determining the zero point. If the ratio is below one, it indicates the presence of a continuous sublayer with the zero-point positioned on it. Conversely, if the ratio exceeds one, there is an absence of a continuous sublayer, and the probable cause for this inconsistency lies in the unique characteristics of the AFM technique when assessing height differentials. While the height of a distinct protrusion on a level surface is ascertained with utmost precision, the depth of a minor crevice between islands is subject to considerable error due to the relatively large tip diameter and the occurrence of lateral flows around its edges.

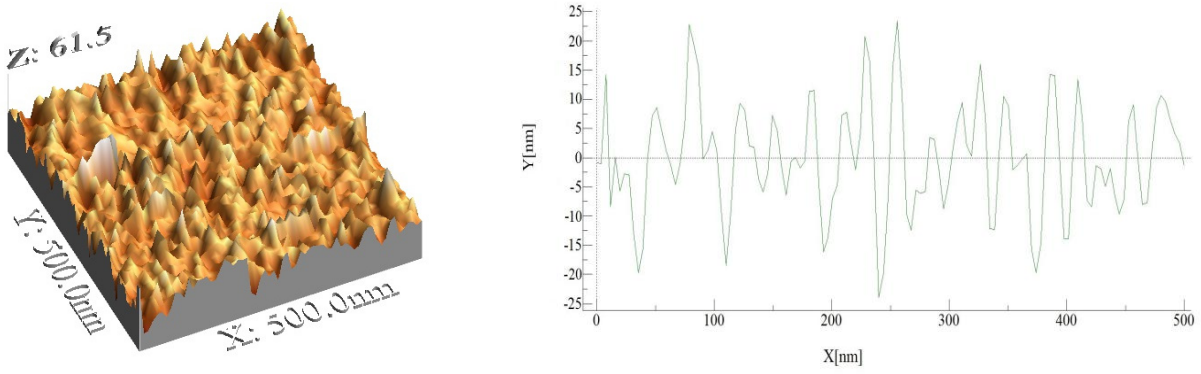

Figure 3. Topography and surface relief of metal oxide films $ZnO_{1-x}S_x$: a - 3D surface image and b - profile along the selected direction.

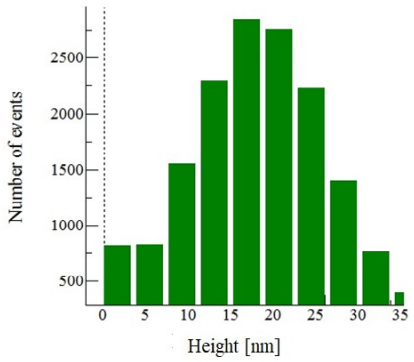

Figure 4. Distribution of islands by height in the array of nanoislands of $ZnO_{1-x}S_x$ films.

Figure 3 illustrates three-dimensional (a) and one-dimensional (b) AFM images of nanostructures formation during the deposition process with an average height of nanostructures ranging from 30 to 50 nm. In Figure 3a, it can be observed that the film surface consists of an array of nanoislands, and the height distribution profile along the direction indicated by the line in Figure 3 is shown in Figure 4.

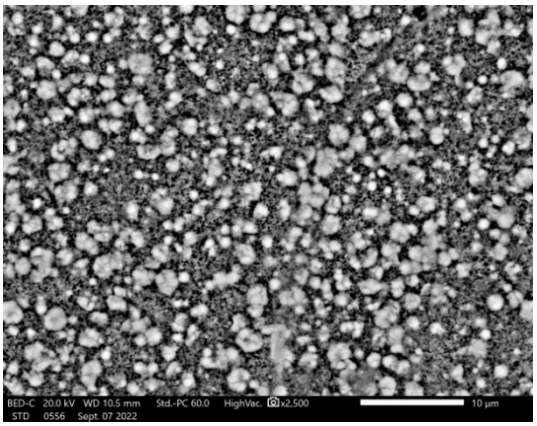

Figure 5. SEM image of the surface of the o synthesized $ZnO_{1-x}S_x$ films

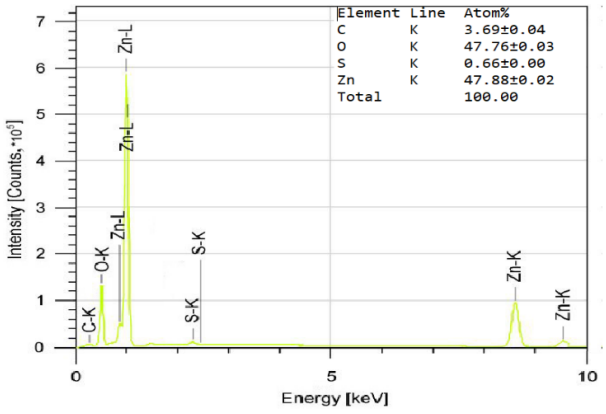

Figure 6. Energy dispersive spectroscopy (EDS) image of the synthesized $ZnO_{1-x}S_x$ films

The distribution of nanoislands presented in Figure 4 reveals that approximately half of the nanostructures have heights ranging from 15 to 25 nm, indicating a significant uniformity of the islands. Furthermore, from the experimental results of the AFM studies, the average density of nanoislands was determined to be 2.9×10^{11} cm^{-2}.

The relief and energy dispersive X-ray spectra (EDS) of the obtained $ZnO_{1-x}S_x$ metal oxide layers were investigated using scanning electron microscopy (SEM), JSM-IT200 (JEOL).

Figure 5 illustrates the SEM image of the surface of the obtained $ZnO_{1-x}S_x$ films. It is evident that the deposition of the films on Si results in the formation of densely packed nanocrystals of $ZnO_{1-x}S_x$ with various geometric shapes and sizes, possibly belonging to the F43m space group. The thickness of the grown layer is 400 nm, and the diameter of $ZnO_{1-x}S_x$ ZnO nanocrystals ranges from 50 to 200 nm. They grow perpendicular to the substrate along the z-axis, and the obtained ZnO films are highly ordered with a high degree of perfection (Fig. 5). The energy dispersive spectroscopy view of the film is presented in Fig. 6. From the analysis of these data, the atomic content of Zn, O, S, and C depending on the thickness of the obtained film has been determined. These show that the atomic content of Zn, O, S, and C has distributions in the following relative magnitudes of 0.4989, 0.4543, 0.0366, and 0.0101 in the near-surface region of the film, respectively.

4. CONCLUSIONS

Consequently, we have successfully fabricated thin films of zinc oxide doped with acceptor impurities consisting of cerium atoms on silicon substrates using the ultrasonic spray pyrolysis method. An advantage of this approach is its cost-effectiveness and the potential for a homogeneous deposition of semiconductor films across large areas without compromising quality, thereby facilitating the future utilization of this technique in semiconductor manufacturing. Atomic force microscopy studies of the metal-cased films showed that during the formation of nanoislands with an average height of about 30-50 nm and densities of 2.9×10^{11} cm^{-2}. SEM data indicate that the thickness of the grown layer is approximately 400 nm, and the diameter of $ZnO_{1-x}S_x$ nanocrystals ranges from 50 to 200 nm, growing perpendicular to the substrate along the z-axis with a crystallographic orientation of (111). It has been determined that the atomic content of Zn, O, S, and C has distributions in the following relative magnitudes of 0.4989, 0.4543, 0.0366, and 0.0101 in the near-surface region of the film.

Conflict of Interests

The authors declare that they have no conflict of interests

Funding

The work was carried out using project funds allocated according to the order of the rector of Andijan State University dated February 7, 2024, No. 04-12.

ORCID

Sirajidin S. Zainabidinov, https://orcid.org/0000-0003-2943-5844; **A.Y. Boboev**, https://orcid.org/0000-0002-3963-708X
Nuritdin Y. Yunusaliyev, https://orcid.org/0000-0003-3766-5420; **Jakhongir N. Usmonov,** https://orcid.org/0000-0002-7243-4938

REFERENCES

[1] S. Nandi, S. Kumar, and A. Misra, "Zinc oxide heterostructures: advances in devices from self-powered photodetectors to self-charging supercapacitors," Mater. Adv. **2**, 6768-6799 (2021). https://doi.org/10.1039/D1MA00670C
[2] V. Karpyna *at. al*., "Zinc oxide – analogue of GaN with new perspective possibilities," Cryst. Res. Technol. **39**(11), 980-992 (2004). https://doi.org/10.1002/crat.200310283
[3] P. Ščajev, and D. Gogova, "Long-lived excitons in thermally annealed hydrothermal ZnO," Heliyon, **10**(4), e26049 (2024). https://doi.org/10.1016/j.heliyon.2024.e26049
[4] I. Ayoub, *et al.,* "Advances in ZnO: Manipulation of defects for enhancing their technological potentials," Nanotechnology Reviews, **11(**1), 575-619 (2022). https://doi.org/10.1515/ntrev-2022-0035
[5] Sh.U. Yuldashev, R.A. Nusretov, I.V. Khvan, V.Sh. Yalishev, and T.W. Kang, "White light emission from ZnO/$Zn_{0.9}Mg_{0.1}O$ heterostrustures grown on Si substrates," Japan. Appl. Phys. **47**(17), 133-135 (2008). https://doi.org/10.1143/JJAP.47.133
[6] S. Zaynabidinov, Sh. Yuldashev, A. Boboev, and N. Yunusaliyev, "X-ray diffraction and electron microscopic studies of the ZnO(S) metal oxide films obtained by the ultrasonic spray pyrolysis method," Herald of the Bauman Moscow State Technical University, Series Natural Sciences, **1**(112), 78-92 (2024). https://doi.org/10.18698/1812-3368-2024-1-78-92
[7] J.M. Bian, X.M. Li, C.Y. Zhang, W.D. Yu, and X.D. Gao, "p-type ZnO films by monodoping of nitrogen and ZnO-based p–n homojunctions," Appl. Phys. Lett, **85**, 4070-4072 (2004). https://doi.org/10.1063/1.1808229
[8] Y. Ryu, *et al*., "Synthesis of p-type ZnO films," Journal of Crystal Growth, **216**(1), 330-334 (200). http://dx.doi.org/10.1016/S0022-0248(00)00437-1
[9] K. Salima, and W. Azzaoui, "Physical properties of spray pyrolysed ZnO thin films obtained from nitrate, acetate and chloride precursors: Comparative study for Solar Cell Applications," Revista Mexicana de Fisica, **69**, 031002 (2023). https://doi.org/10.31349/RevMexFis.69.031002
[10] R. Kumar, M. Sekhar, Raghvendra, R. Laha, and S. Pandey, "Comparative studies of ZnO thin films grown by electron beam evaporation, pulsed laser and RF sputtering technique for optoelectronics applications," Applied Physics, **126**, 859 (2020). https://doi.org/10.1007/s00339-020-04046-8
[11] S.Z. Zaynabidinov, A.Y. Boboev, and N.Y. Yunusaliyev, "Effect of γ-irradiation on structure and electrophysical properties of S-doped Zno films," East European Journal of Physics, (2), 321-326 (2024). https://doi.org/10.26565/2312-4334-2024-2-37.
[12] E. Ahmed, M. Samy, and L. Saad "Highly Conductive N-type Aluminum Dopped Zinc Oxide for CZTS Kieserite Solar Cell," Egypt. J. Chem. **67**(4), 309-313 (2024). https://doi.org/10.21608/ejchem.2023.241700.8724

ОПТИМІЗОВАНИЙ ПРИСТРІЙ УЛЬТРАЗВУКОВОГО СПРЕЙ-ПІРОЛІЗУ ДЛЯ ВИРОБНИЦТВА МЕТАЛОКСИДНИХ ПЛІВОК ТА ЇХ МОРФОЛОГІЯ

Сіражідін С. Зайнабіднов[a], Акрамжон Ю. Бобоєв[a,b], Нурітдін Ю. Юнусалієв[a], Джахонгір Н. Усмонов[a]

[a]*Андижанський державний університет імені З.М. Бабур, Андижан, Узбекистан*

[b]*Інститут фізики напівпровідників та мікроелектроніки Національного університету Узбекистану, Ташкент, Узбекистан*

У цій роботі ми розробили оптимізоване пристрій ультразвукового розпилювального піролізу для отримання плівок оксидів металів. Ключова перевага цього обладнання полягає в його економічній ефективності та здатності послідовно покривати великі поверхні без шкоди для цілісності напівпровідникових плівок, таким чином оптимізуючи процес виробництва напівпровідникових плівок. Отримані плівки демонструють такі властивості: товщина нанесеного шару становить приблизно 400 нм, тоді як діаметр нанокристалів $ZnO_{1-x}S_x$ коливається від 50 до 200 нм, орієнтованих перпендикулярно до кристалографічної орієнтації (111). Під час виробництва наностріжнів середня висота оцінюється приблизно в 30-50 нм із зазначеною щільністю $2{,}9\times10^{11}$ см$^{-2}$.

Ключові слова: плівка*; просторова група; субкристал; нанокристал; ефект квантового розміру; параметр решітки; прозора електроніка; щілина*